

Measurement of the $B^\pm \rightarrow \rho^\pm \pi^0$ Branching Fraction and Direct CP Asymmetry

The *BABAR* Collaboration

October 26, 2018

Abstract

An improved measurement of the process $B^\pm \rightarrow \rho^\pm \pi^0$ is presented. The data sample of 211 fb^{-1} comprises 232 million $\Upsilon(4S) \rightarrow B\bar{B}$ decays collected with the *BABAR* detector at the PEP-II asymmetric B Factory at SLAC. The yield and CP asymmetry are calculated using an extended maximum likelihood fitting method. The branching fraction and asymmetry are found to be $\mathcal{B}(B^\pm \rightarrow \rho^\pm \pi^0) = [10.0 \pm 1.4 (\text{Stat.}) \pm 0.9 (\text{Syst.})] \times 10^{-6}$ and $\mathcal{A}_{CP}(B^\pm \rightarrow \rho^\pm \pi^0) = -0.01 \pm 0.13 (\text{Stat.}) \pm 0.02 (\text{Syst.})$, superseding previous measurements. The statistical significance of the signal is calculated to be 8.7σ .

Contributed to the XXIIst International Symposium on Lepton and Photon Interactions at High Energies, 6/30 — 7/5/2005, Uppsala, Sweden

Stanford Linear Accelerator Center, Stanford University, Stanford, CA 94309

Work supported in part by Department of Energy contract DE-AC03-76SF00515.

The BABAR Collaboration,

B. Aubert, R. Barate, D. Boutigny, F. Couderc, Y. Karyotakis, J. P. Lees, V. Poireau, V. Tisserand,
A. Zghiche

Laboratoire de Physique des Particules, F-74941 Annecy-le-Vieux, France

E. Grauges

IFAE, Universitat Autònoma de Barcelona, E-08193 Bellaterra, Barcelona, Spain

A. Palano, M. Pappagallo, A. Pompili

Università di Bari, Dipartimento di Fisica and INFN, I-70126 Bari, Italy

J. C. Chen, N. D. Qi, G. Rong, P. Wang, Y. S. Zhu

Institute of High Energy Physics, Beijing 100039, China

G. Eigen, I. Ofte, B. Stugu

University of Bergen, Institute of Physics, N-5007 Bergen, Norway

G. S. Abrams, M. Battaglia, A. B. Breon, D. N. Brown, J. Button-Shafer, R. N. Cahn, E. Charles,
C. T. Day, M. S. Gill, A. V. Gritsan, Y. Groyzman, R. G. Jacobsen, R. W. Kadel, J. Kadyk, L. T. Kerth,
Yu. G. Kolomensky, G. Kukartsev, G. Lynch, L. M. Mir, P. J. Oddone, T. J. Orimoto, M. Pripstein,
N. A. Roe, M. T. Ronan, W. A. Wenzel

Lawrence Berkeley National Laboratory and University of California, Berkeley, California 94720, USA

M. Barrett, K. E. Ford, T. J. Harrison, A. J. Hart, C. M. Hawkes, S. E. Morgan, A. T. Watson

University of Birmingham, Birmingham, B15 2TT, United Kingdom

M. Fritsch, K. Goetzen, T. Held, H. Koch, B. Lewandowski, M. Pelizaeus, K. Peters, T. Schroeder,
M. Steinke

Ruhr Universität Bochum, Institut für Experimentalphysik 1, D-44780 Bochum, Germany

J. T. Boyd, J. P. Burke, N. Chevalier, W. N. Cottingham

University of Bristol, Bristol BS8 1TL, United Kingdom

T. Cuhadar-Donszelmann, B. G. Fulsom, C. Hearty, N. S. Knecht, T. S. Mattison, J. A. McKenna

University of British Columbia, Vancouver, British Columbia, Canada V6T 1Z1

A. Khan, P. Kyberd, M. Saleem, L. Teodorescu

Brunel University, Uxbridge, Middlesex UB8 3PH, United Kingdom

A. E. Blinov, V. E. Blinov, A. D. Bukin, V. P. Druzhinin, V. B. Golubev, E. A. Kravchenko,
A. P. Onuchin, S. I. Serednyakov, Yu. I. Skovpen, E. P. Solodov, A. N. Yushkov

Budker Institute of Nuclear Physics, Novosibirsk 630090, Russia

D. Best, M. Bondioli, M. Bruinsma, M. Chao, S. Curry, I. Eschrich, D. Kirkby, A. J. Lankford, P. Lund,
M. Mandelkern, R. K. Mommsen, W. Roethel, D. P. Stoker

University of California at Irvine, Irvine, California 92697, USA

C. Buchanan, B. L. Hartfiel, A. J. R. Weinstein

University of California at Los Angeles, Los Angeles, California 90024, USA

- S. D. Foulkes, J. W. Gary, O. Long, B. C. Shen, K. Wang, L. Zhang
University of California at Riverside, Riverside, California 92521, USA
- D. del Re, H. K. Hadavand, E. J. Hill, D. B. MacFarlane, H. P. Paar, S. Rahatlou, V. Sharma
University of California at San Diego, La Jolla, California 92093, USA
- J. W. Berryhill, C. Campagnari, A. Cunha, B. Dahmes, T. M. Hong, M. A. Mazur, J. D. Richman,
W. Verkerke
University of California at Santa Barbara, Santa Barbara, California 93106, USA
- T. W. Beck, A. M. Eisner, C. J. Flacco, C. A. Heusch, J. Kroseberg, W. S. Lockman, G. Nesom, T. Schalk,
B. A. Schumm, A. Seiden, P. Spradlin, D. C. Williams, M. G. Wilson
University of California at Santa Cruz, Institute for Particle Physics, Santa Cruz, California 95064, USA
- J. Albert, E. Chen, G. P. Dubois-Felsmann, A. Dvoretzskii, D. G. Hitlin, I. Narsky, T. Piatenko,
F. C. Porter, A. Ryd, A. Samuel
California Institute of Technology, Pasadena, California 91125, USA
- R. Andreassen, S. Jayatilleke, G. Mancinelli, B. T. Meadows, M. D. Sokoloff
University of Cincinnati, Cincinnati, Ohio 45221, USA
- F. Blanc, P. Bloom, S. Chen, W. T. Ford, J. F. Hirschauer, A. Kreisel, U. Nauenberg, A. Olivas,
P. Rankin, W. O. Ruddick, J. G. Smith, K. A. Ulmer, S. R. Wagner, J. Zhang
University of Colorado, Boulder, Colorado 80309, USA
- A. Chen, E. A. Eckhart, J. L. Harton, A. Soffer, W. H. Toki, R. J. Wilson, Q. Zeng
Colorado State University, Fort Collins, Colorado 80523, USA
- D. Altenburg, E. Feltresi, A. Hauke, B. Spaan
Universität Dortmund, Institut für Physik, D-44221 Dortmund, Germany
- T. Brandt, J. Brose, M. Dickopp, V. Klose, H. M. Lacker, R. Nogowski, S. Otto, A. Petzold, G. Schott,
J. Schubert, K. R. Schubert, R. Schwierz, J. E. Sundermann
Technische Universität Dresden, Institut für Kern- und Teilchenphysik, D-01062 Dresden, Germany
- D. Bernard, G. R. Bonneaud, P. Grenier, S. Schrenk, Ch. Thiebaux, G. Vasileiadis, M. Verderi
Ecole Polytechnique, LLR, F-91128 Palaiseau, France
- D. J. Bard, P. J. Clark, W. Gradl, F. Muheim, S. Playfer, Y. Xie
University of Edinburgh, Edinburgh EH9 3JZ, United Kingdom
- M. Andreotti, V. Azzolini, D. Bettoni, C. Bozzi, R. Calabrese, G. Cibinetto, E. Luppi, M. Negrini,
L. Piemontese
Università di Ferrara, Dipartimento di Fisica and INFN, I-44100 Ferrara, Italy
- F. Anulli, R. Baldini-Ferrolì, A. Calcaterra, R. de Sangro, G. Finocchiaro, P. Patteri, I. M. Peruzzi,¹
M. Piccolo, A. Zallo
Laboratori Nazionali di Frascati dell'INFN, I-00044 Frascati, Italy

¹Also with Università di Perugia, Dipartimento di Fisica, Perugia, Italy

A. Buzzo, R. Capra, R. Contri, M. Lo Vetere, M. Macri, M. R. Monge, S. Passaggio, C. Patrignani,
E. Robutti, A. Santroni, S. Tosi

Università di Genova, Dipartimento di Fisica and INFN, I-16146 Genova, Italy

G. Brandenburg, K. S. Chaisanguanthum, M. Morii, E. Won, J. Wu

Harvard University, Cambridge, Massachusetts 02138, USA

R. S. Dubitzky, U. Langenegger, J. Marks, S. Schenk, U. Uwer

Universität Heidelberg, Physikalisches Institut, Philosophenweg 12, D-69120 Heidelberg, Germany

W. Bhimji, D. A. Bowerman, P. D. Dauncey, U. Egede, R. L. Flack, J. R. Gaillard, G. W. Morton,
J. A. Nash, M. B. Nikolich, G. P. Taylor, W. P. Vazquez

Imperial College London, London, SW7 2AZ, United Kingdom

M. J. Charles, W. F. Mader, U. Mallik, A. K. Mohapatra

University of Iowa, Iowa City, Iowa 52242, USA

J. Cochran, H. B. Crawley, V. Eyges, W. T. Meyer, S. Prell, E. I. Rosenberg, A. E. Rubin, J. Yi

Iowa State University, Ames, Iowa 50011-3160, USA

N. Arnaud, M. Davier, X. Giroux, G. Grosdidier, A. Höcker, F. Le Diberder, V. Lepeltier, A. M. Lutz,
A. Oyanguren, T. C. Petersen, M. Pierini, S. Plaszczynski, S. Rodier, P. Roudeau, M. H. Schune,

A. Stocchi, G. Wormser

Laboratoire de l'Accélérateur Linéaire, F-91898 Orsay, France

C. H. Cheng, D. J. Lange, M. C. Simani, D. M. Wright

Lawrence Livermore National Laboratory, Livermore, California 94550, USA

A. J. Bevan, C. A. Chavez, I. J. Forster, J. R. Fry, E. Gabathuler, R. Gamet, K. A. George,
D. E. Hutchcroft, R. J. Parry, D. J. Payne, K. C. Schofield, C. Touramanis

University of Liverpool, Liverpool L69 7ZE, United Kingdom

C. M. Cormack, F. Di Lodovico, W. Menges, R. Sacco

Queen Mary, University of London, E1 4NS, United Kingdom

C. L. Brown, G. Cowan, H. U. Flaecher, M. G. Green, D. A. Hopkins, P. S. Jackson, T. R. McMahon,
S. Ricciardi, F. Salvatore

University of London, Royal Holloway and Bedford New College, Egham, Surrey TW20 0EX, United Kingdom

D. Brown, C. L. Davis

University of Louisville, Louisville, Kentucky 40292, USA

J. Allison, N. R. Barlow, R. J. Barlow, C. L. Edgar, M. C. Hodgkinson, M. P. Kelly, G. D. Lafferty,
M. T. Naisbit, J. C. Williams

University of Manchester, Manchester M13 9PL, United Kingdom

C. Chen, W. D. Hulsbergen, A. Jawahery, D. Kovalskyi, C. K. Lae, D. A. Roberts, G. Simi

University of Maryland, College Park, Maryland 20742, USA

G. Blaylock, C. Dallapiccola, S. S. Hertzbach, R. Kofler, V. B. Koptchev, X. Li, T. B. Moore, S. Saremi,
H. Staengle, S. Willocq

University of Massachusetts, Amherst, Massachusetts 01003, USA

R. Cowan, K. Koeneke, G. Sciolla, S. J. Sekula, M. Spitznagel, F. Taylor, R. K. Yamamoto
*Massachusetts Institute of Technology, Laboratory for Nuclear Science, Cambridge, Massachusetts 02139,
USA*

H. Kim, P. M. Patel, S. H. Robertson

McGill University, Montréal, Quebec, Canada H3A 2T8

A. Lazzaro, V. Lombardo, F. Palombo

Università di Milano, Dipartimento di Fisica and INFN, I-20133 Milano, Italy

J. M. Bauer, L. Cremaldi, V. Eschenburg, R. Godang, R. Kroeger, J. Reidy, D. A. Sanders, D. J. Summers,
H. W. Zhao

University of Mississippi, University, Mississippi 38677, USA

S. Brunet, D. Côté, P. Taras, B. Viaud

Université de Montréal, Laboratoire René J. A. Lévesque, Montréal, Quebec, Canada H3C 3J7

H. Nicholson

Mount Holyoke College, South Hadley, Massachusetts 01075, USA

N. Cavallo,² G. De Nardo, F. Fabozzi,² C. Gatto, L. Lista, D. Monorchio, P. Paolucci, D. Piccolo,
C. Sciacca

Università di Napoli Federico II, Dipartimento di Scienze Fisiche and INFN, I-80126, Napoli, Italy

M. Baak, H. Bulten, G. Raven, H. L. Snoek, L. Wilden

*NIKHEF, National Institute for Nuclear Physics and High Energy Physics, NL-1009 DB Amsterdam, The
Netherlands*

C. P. Jessop, J. M. LoSecco

University of Notre Dame, Notre Dame, Indiana 46556, USA

T. Allmendinger, G. Benelli, K. K. Gan, K. Honscheid, D. Hufnagel, P. D. Jackson, H. Kagan, R. Kass,
T. Pulliam, A. M. Rahimi, R. Ter-Antonyan, Q. K. Wong

Ohio State University, Columbus, Ohio 43210, USA

J. Brau, R. Frey, O. Igonkina, M. Lu, C. T. Potter, N. B. Sinev, D. Strom, J. Strube, E. Torrence

University of Oregon, Eugene, Oregon 97403, USA

F. Galeazzi, M. Margoni, M. Morandin, M. Posocco, M. Rotondo, F. Simonetto, R. Stroili, C. Voci

Università di Padova, Dipartimento di Fisica and INFN, I-35131 Padova, Italy

M. Benayoun, H. Briand, J. Chauveau, P. David, L. Del Buono, Ch. de la Vaissière, O. Hamon,
M. J. J. John, Ph. Leruste, J. Malclès, J. Ocariz, L. Roos, G. Therin

*Universités Paris VI et VII, Laboratoire de Physique Nucléaire et de Hautes Energies, F-75252 Paris,
France*

²Also with Università della Basilicata, Potenza, Italy

P. K. Behera, L. Gladney, Q. H. Guo, J. Panetta
University of Pennsylvania, Philadelphia, Pennsylvania 19104, USA

M. Biasini, R. Covarelli, S. Pacetti, M. Pioppi
Università di Perugia, Dipartimento di Fisica and INFN, I-06100 Perugia, Italy

C. Angelini, G. Batignani, S. Bettarini, F. Bucci, G. Calderini, M. Carpinelli, R. Cenci, F. Forti,
M. A. Giorgi, A. Lusiani, G. Marchiori, M. Morganti, N. Neri, E. Paoloni, M. Rama, G. Rizzo, J. Walsh
Università di Pisa, Dipartimento di Fisica, Scuola Normale Superiore and INFN, I-56127 Pisa, Italy

M. Haire, D. Judd, D. E. Wagoner
Prairie View A&M University, Prairie View, Texas 77446, USA

J. Biesiada, N. Danielson, P. Elmer, Y. P. Lau, C. Lu, J. Olsen, A. J. S. Smith, A. V. Telnov
Princeton University, Princeton, New Jersey 08544, USA

F. Bellini, G. Cavoto, A. D’Orazio, E. Di Marco, R. Faccini, F. Ferrarotto, F. Ferroni, M. Gaspero, L. Li
Gioi, M. A. Mazzoni, S. Morganti, G. Piredda, F. Polci, F. Safai Tehrani, C. Voena
Università di Roma La Sapienza, Dipartimento di Fisica and INFN, I-00185 Roma, Italy

H. Schröder, G. Wagner, R. Waldi
Universität Rostock, D-18051 Rostock, Germany

T. Adye, N. De Groot, B. Franek, G. P. Gopal, E. O. Olaiya, F. F. Wilson
Rutherford Appleton Laboratory, Chilton, Didcot, Oxon, OX11 0QX, United Kingdom

R. Aleksan, S. Emery, A. Gaidot, S. F. Ganzhur, P.-F. Giraud, G. Graziani, G. Hamel de Monchenault,
W. Kozanecki, M. Legendre, G. W. London, B. Mayer, G. Vasseur, Ch. Yèche, M. Zito
DSM/Dapnia, CEA/Saclay, F-91191 Gif-sur-Yvette, France

M. V. Purohit, A. W. Weidemann, J. R. Wilson, F. X. Yumiceva
University of South Carolina, Columbia, South Carolina 29208, USA

T. Abe, M. T. Allen, D. Aston, N. van Bakel, R. Bartoldus, N. Berger, A. M. Boyarski, O. L. Buchmueller,
R. Claus, J. P. Coleman, M. R. Convery, M. Cristinziani, J. C. Dingfelder, D. Dong, J. Dorfan, D. Dujmic,
W. Dunwoodie, S. Fan, R. C. Field, T. Glanzman, S. J. Gowdy, T. Hadig, V. Halyo, C. Hast, T. Hryn’ova,
W. R. Innes, M. H. Kelsey, P. Kim, M. L. Kocian, D. W. G. S. Leith, J. Libby, S. Luitz, V. Luth,
H. L. Lynch, H. Marsiske, R. Messner, D. R. Muller, C. P. O’Grady, V. E. Ozcan, A. Perazzo, M. Perl,
B. N. Ratcliff, A. Roodman, A. A. Salnikov, R. H. Schindler, J. Schwiening, A. Snyder, J. Stelzer, D. Su,
M. K. Sullivan, K. Suzuki, S. Swain, J. M. Thompson, J. Va’vra, M. Weaver, W. J. Wisniewski,
M. Wittgen, D. H. Wright, A. K. Yarritu, K. Yi, C. C. Young
Stanford Linear Accelerator Center, Stanford, California 94309, USA

P. R. Burchat, A. J. Edwards, S. A. Majewski, B. A. Petersen, C. Roat
Stanford University, Stanford, California 94305-4060, USA

M. Ahmed, S. Ahmed, M. S. Alam, J. A. Ernst, M. A. Saeed, F. R. Wappler, S. B. Zain
State University of New York, Albany, New York 12222, USA

W. Bugg, M. Krishnamurthy, S. M. Spanier
University of Tennessee, Knoxville, Tennessee 37996, USA

R. Eckmann, J. L. Ritchie, A. Satpathy, R. F. Schwitters
University of Texas at Austin, Austin, Texas 78712, USA

J. M. Izen, I. Kitayama, X. C. Lou, S. Ye
University of Texas at Dallas, Richardson, Texas 75083, USA

F. Bianchi, M. Bona, F. Gallo, D. Gamba
Università di Torino, Dipartimento di Fisica Sperimentale and INFN, I-10125 Torino, Italy

M. Bomben, L. Bosisio, C. Cartaro, F. Cossutti, G. Della Ricca, S. Dittongo, S. Grancagnolo, L. Lanceri,
L. Vitale

Università di Trieste, Dipartimento di Fisica and INFN, I-34127 Trieste, Italy

F. Martinez-Vidal
IFIC, Universitat de Valencia-CSIC, E-46071 Valencia, Spain

R. S. Panvini³
Vanderbilt University, Nashville, Tennessee 37235, USA

Sw. Banerjee, B. Bhuyan, C. M. Brown, D. Fortin, K. Hamano, R. Kowalewski, J. M. Roney, R. J. Sobie
University of Victoria, Victoria, British Columbia, Canada V8W 3P6

J. J. Back, P. F. Harrison, T. E. Latham, G. B. Mohanty
Department of Physics, University of Warwick, Coventry CV4 7AL, United Kingdom

H. R. Band, X. Chen, B. Cheng, S. Dasu, M. Datta, A. M. Eichenbaum, K. T. Flood, M. Graham,
J. J. Hollar, J. R. Johnson, P. E. Kutter, H. Li, R. Liu, B. Mellado, A. Mihalyi, Y. Pan, R. Prepost,
P. Tan, J. H. von Wimmersperg-Toeller, S. L. Wu, Z. Yu
University of Wisconsin, Madison, Wisconsin 53706, USA

H. Neal
Yale University, New Haven, Connecticut 06511, USA

³Deceased

1 Introduction

Branching fraction and CP asymmetry measurements of charmless B meson decays provide valuable constraints for the determination of the unitarity triangle constructed from elements of the Cabibbo-Kobayashi-Maskawa quark-mixing matrix [1, 2]. In particular, the angle $\alpha \equiv \arg[-V_{td}V_{tb}^*/V_{ud}V_{ub}^*]$ of the unitarity triangle can be extracted from decays of the B meson to $\rho^\pm\pi^\mp$ final states [3]. However, the extraction is complicated by the interference of decay amplitudes with differing weak and strong phases. One strategy to overcome this problem is to perform an $SU(2)$ analysis that uses all $\rho\pi$ final states [4]. Assuming isospin symmetry, the angle α can be determined free of hadronic uncertainties from a pentagon relation formed in the complex plane by the five decay amplitudes $B^0 \rightarrow \rho^+\pi^-$, $B^0 \rightarrow \rho^-\pi^+$, $B^0 \rightarrow \rho^0\pi^0$, $B^+ \rightarrow \rho^+\pi^0$ and $B^+ \rightarrow \rho^0\pi^+$. These amplitudes can be determined from measurements of the corresponding decay rates and CP asymmetries. While all these modes have been measured, the current experimental uncertainties need to be reduced substantially for a determination of α . Here we present an update to a previous measurement [5] of the $B^\pm \rightarrow \rho^\pm\pi^0$ branching fraction and CP asymmetry

$$A_{CP} = \frac{N(B^- \rightarrow \rho^- \pi^0) - N(B^+ \rightarrow \rho^+ \pi^0)}{N(B^- \rightarrow \rho^- \pi^0) + N(B^+ \rightarrow \rho^+ \pi^0)}.$$

2 Data Set and Candidate Selection

The data used in this analysis were collected with the *BABAR* detector [6] at the PEP-II asymmetric-energy e^+e^- storage ring at SLAC. Charged-particle trajectories are measured by a five-layer double-sided silicon vertex tracker and a 40-layer drift chamber located within a 1.5-T solenoidal magnetic field. Charged hadrons are identified by combining energy-loss information from tracking with the measurements from a ring-imaging Cherenkov detector. Photons are detected by a CsI(Tl) crystal electromagnetic calorimeter with an energy resolution of $\sigma_E/E = 0.023(E/\text{GeV})^{-1/4} \oplus 0.014$. The magnetic flux return is instrumented for muon and K_L^0 identification.

The data sample includes 232 ± 3 million $B\bar{B}$ pairs collected at the $\Upsilon(4S)$ resonance, corresponding to an integrated luminosity of 211 fb^{-1} . It is assumed that neutral and charged B meson pairs are produced in equal numbers [7]. In addition, 22 fb^{-1} of data collected 40 MeV below the $\Upsilon(4S)$ resonance mass are used for background studies.

We perform full detector Monte Carlo (MC) simulations equivalent to 460 fb^{-1} of generic $B\bar{B}$ decays and 140 fb^{-1} of continuum quark-antiquark production events. In addition, we simulate over 50 exclusive charmless B decay modes, including 1.4 million signal $B^\pm \rightarrow \rho^\pm\pi^0$ decays.

B meson candidates are reconstructed from one charged track and two neutral pions, with the following requirements:

Track quality. The charged track used to form the $B^\pm \rightarrow \rho^\pm\pi^0$ candidate is required to have at least 12 hits in the drift chamber, to have a transverse momentum greater than 0.1 GeV/c, and to be consistent with originating from a B -meson decay. Its signal in the tracking and Cherenkov detectors is required to be consistent with that of a pion. We remove tracks that pass electron selection criteria based on dE/dx and calorimeter information.

π^0 quality. Neutral pion candidates are formed from two photons, each with a minimum energy of 0.03 GeV and a lateral moment [8] of their shower energy deposition greater than zero and less than 0.6. The angular acceptance of photons is restricted to exclude parts of the calorimeter where showers are not fully contained. We require the photon clusters forming the π^0 to be separated in space, with a π^0 energy of at least 0.2 GeV and an invariant mass between 0.10 and 0.16 GeV/c².

Kinematic requirements. Two kinematic variables, $\Delta E = E_B^* - \sqrt{s}/2$ and the beam energy substituted mass of the B -meson $m_{\text{ES}} = \sqrt{(s/2 + \mathbf{p}_0 \cdot \mathbf{p}_B)^2/E_0^2 - \mathbf{p}_B^2}$, are used for the final selection of events. Here E_B^* is the energy of the B meson candidate in the center-of-mass frame, E_0 and \sqrt{s} are the total energies of the e^+e^- system in the laboratory and center-of-mass frames, respectively; \mathbf{p}_0 and \mathbf{p}_B are the three-momenta of the e^+e^- system and the B candidate in the laboratory frame, respectively. For correctly reconstructed $\rho^\pm\pi^0$ candidates ΔE peaks at zero, while final states with a charged kaon, such as $B^\pm \rightarrow K^{*\pm}\pi^0$, shift ΔE by approximately 80 MeV on average. Events are selected with $5.20 < m_{\text{ES}} < 5.29$ GeV/ c^2 and $|\Delta E| < 0.20$ GeV. The ΔE limits help remove background from two- and four-body B decays at a small cost to signal efficiency.

Continuum suppression. Continuum quark-antiquark production is the dominant background. To suppress it, we select only those events where the angle θ_{Sph}^B in the center-of-mass frame between the direction of the B meson candidate and the sphericity axis of the rest of the event satisfies $|\cos \theta_{\text{Sph}}^B| < 0.9$. In addition, we construct a non-linear discriminant, implemented as an artificial neural network, that uses three input parameters: the zeroth- and second-order Legendre event shape polynomials L_0, L_2 calculated from the momenta and polar angles of all charged particle and photon candidates not associated with the B meson candidate, and the output of a multivariate, non-linear B meson candidate tagging algorithm [9]. The output ANN of the artificial neural network is peaked at 0.5 for continuum-like events and at 1.0 for B decays. We require $ANN > 0.63$ for our event selection.

ρ mass window. To further improve the signal-to-background ratio we restrict the invariant mass of the ρ candidate to $0.55 < m_{\pi\pi} < 0.95$ GeV/ c^2 .

Multiple candidates. Neutral pion combinatorics can lead to more than one B -meson candidate per event. We choose the best candidate based on a χ^2 formed from the measured masses of the two π^0 candidates within the event compared to the known π^0 mass [10]. In the case of multiple charged pion candidates the choice is random.

Efficiency. The total $B^\pm \rightarrow \rho^\pm\pi^0$ selection efficiency is $15.4 \pm 0.1\%$. In MC studies, the signal candidate is correctly reconstructed 54.9% of the time. The remaining candidates come from self-cross-feed (SCF, 37.5%) and mistag events (7.6%). We define SCF events as those where one or more elements of the B -candidate reconstruction are incorrect except for its charge. They stem primarily from swapping the low energy π^0 from the resonance with another from the rest of the event. Signal events reconstructed with the wrong charge are classified as mistag events. Both SCF and mistag events emulate signal events, however the resolution in m_{ES} and ΔE tends to be worse.

3 Background Contributions

MC events are used to study backgrounds from other B -meson decays. The dominant contribution comes from $b \rightarrow c$ transitions; the next most important is from charmless B -meson decays. The latter tend to be more problematic as the branching fractions are often poorly known, and because they may peak at the same invariant mass as the signal $B^\pm \rightarrow \rho^\pm\pi^0$ events. Seventeen individual charmless modes show a significant contribution once the event selection has been applied (Table 1). These modes are added into the fit fixed at the yield and asymmetry determined by the simulation, given an assumed branching fraction. Wherever branching fractions are not available, we use half the upper limit. If no charge asymmetry measurement is available, we assume zero asymmetry.

ρ^* resonances. Although all other states which decay like the ρ to $\pi\pi^0$ – subsequently referred

Backgrounds to $\rho^\pm\pi^0$ from B -related Sources				
Mode	Efficiency (%)	Assumed \mathcal{B} ($\times 10^{-6}$)	Assumed \mathcal{A}_{CP}	Expected yield
Generic $b \rightarrow c$	1.69×10^{-4}	-	0.00	392.3 ± 19.8
$B^0 \rightarrow \rho^\pm\rho^\mp$	2.12	30.0 ± 6.0 [11]	0.00 ± 0.00	147.7 ± 29.5
$B^0 \rightarrow \rho^\pm\pi^\mp$	2.39	24 ± 2.5 [11]	0.00 ± 0.20	132.9 ± 13.8
$B^\pm \rightarrow \pi^\pm\pi^0$	4.12	5.5 ± 0.6 [11]	-0.02 ± 0.07 [11]	52.5 ± 5.7
$B^0 \rightarrow a_1^0\pi^0$	1.16	17.5 ± 17.5 [5]	0.00 ± 0.20	46.9 ± 46.9
$B^\pm \rightarrow \rho^\pm\rho^0$	0.57	26.4 ± 6.4 [11]	-0.09 ± 0.16 [11]	34.6 ± 8.4
$B^\pm \rightarrow \pi^\pm K_s(\rightarrow \pi^0\pi^0)$	1.49	3.74 ± 0.20 [11]	-0.02 ± 0.03 [11]	12.9 ± 0.7
$B^\pm \rightarrow K^\pm\pi^0$	0.41	12.1 ± 0.8 [11]	0.04 ± 0.04 [11]	11.5 ± 0.8
$B^0 \rightarrow \pi^0\pi^0$	2.62	1.51 ± 0.28 [11]	0.00 ± 0.00	9.2 ± 1.7
$B^0 \rightarrow \eta'\pi^0$	1.15	1.85 ± 1.85 [11]	0.00 ± 0.20	4.9 ± 4.9
$B^\pm \rightarrow \pi^\pm K^{*0}$	0.17	9.76 ± 1.22 [11]	0.00 ± 0.20	3.8 ± 0.5
$B^0 \rightarrow \pi^0 K^{*0}$	0.90	1.7 ± 0.8 [11]	0.00 ± 0.20	3.5 ± 1.7
$B^\pm \rightarrow K^{*\pm}\pi^0$	0.61	2.3 ± 0.8 [12]	0.04 ± 0.29	3.4 ± 1.0
$B^0 \rightarrow K^\pm\rho^\mp$	0.14	9.9 ± 1.6 [11]	0.17 ± 0.16 [11]	3.2 ± 0.5
$B^\pm \rightarrow K^{*\pm}\gamma$	0.02	40.3 ± 2.6 [11]	-0.01 ± 0.03 [11]	2.1 ± 0.1
$B^\pm \rightarrow \rho^\pm\gamma$	0.65	0.9 ± 0.9 [11]	0.00 ± 0.20	1.4 ± 1.4
$B^0 \rightarrow K^{*\pm}\rho^\mp$	0.05	12.0 ± 12.0 [11]	0.00 ± 0.20	1.4 ± 1.4
$B^\pm \rightarrow \rho^\pm(1450)\pi^0$	-	-	0.00 ± 0.20	8 ± 8
Total	-	-	-	872.2 ± 62.1

Table 1: The individual B -background modes considered in the fit. The expected number of events after all cuts are listed for each mode. For modes which do not have well measured branching fractions, half the upper limit is used. If no \mathcal{A}_{CP} measurement is available, we assume zero asymmetry with a 20% uncertainty.

to as ρ^* – lie outside our $\rho(770)$ mass cut, a contribution to our signal cannot be *a priori* ruled out. The only non-strange vector resonances which can decay to two pions are the $\rho(1450)$ and the $\rho(1700)$. To account for the possible presence of these modes, a fit to the $B^\pm \rightarrow \rho^{*\pm}\pi^0$ yield is performed in a sideband of the invariant mass using the three variables m_{ES} , ΔE , and ANN . The mass window is chosen to be as far as possible from the $\rho(770)$ mass, centered near the pole of the $\rho(1700)$ at $1.5 < m_{\pi\pi} < 2.0$ GeV/ c^2 . The fitted yield for the $B^\pm \rightarrow \rho^{*\pm}\pi^0$ decay is then extrapolated into the nominal region. Although the choice of mass range is motivated by the $\rho(1700)$, any yield seen is attributed entirely to the $\rho(1450)$, which is the closer of the two resonances to the signal. From the $B^\pm \rightarrow \rho^\pm(1450)\pi^0$ MC, the ratio of candidates in the sideband to candidates in the signal mass region is approximately 12.6:1. The fit in the sideband yields 101 ± 32 events, resulting in an estimate of the ρ^* background of 8 events. We assign a conservative systematic uncertainty of 100% to this number. The ρ^* then enters into the nominal fit with PDFs constructed from $B^\pm \rightarrow \rho^\pm(1450)\pi^0$ MC simulation.

Non-resonant decays to $\pi^\pm\pi^0\pi^0$. The non-resonant $B^\pm \rightarrow \pi^\pm\pi^0\pi^0$ branching fraction has, to date, not been measured. To estimate the significance of its contribution we select a region of the Dalitz plot — defined by the triangle $(m_{\pi^\pm\pi_1^0}^2, m_{\pi^\pm\pi_2^0}^2) = (6, 6), (6, 15), (11, 11)$ GeV $^2/c^4$ — that is far from the signal as well as $\rho(1450)$ and higher resonances and which has low levels of continuum background. A likelihood fit in this region yields -5.1 ± 7.6 non-resonant events in a data sample of 1100 events. This is consistent with zero. The non-resonant contribution is therefore deemed negligible.

4 The Maximum Likelihood Fit

An unbinned maximum likelihood fit to the variables m_{ES} , ΔE , $m_{\pi\pi}$, and ANN is used to extract the total number of signal $B^\pm \rightarrow \rho^\pm\pi^0$ and continuum background events and their respective charge asymmetries. The likelihood for the selected sample is given by the product of the probability density functions (PDF) for each individual candidate, multiplied by the Poisson factor:

$$\mathcal{L} = \frac{1}{N!} e^{-N'} (N')^N \prod_{i=1}^N \mathcal{P}_i,$$

where N and N' are the number of observed and expected events, respectively. The PDF \mathcal{P}_i for a given event i is the sum of the signal and background terms:

$$\begin{aligned} \mathcal{P}_i &= N^{\text{Sig}} \times \frac{1}{2} [(1 - Q_i A^{\text{Sig}}) f_{\text{Sig}} \mathcal{P}_i^{\text{Sig}} \\ &\quad + (1 - Q_i A^{\text{Sig}}) f_{\text{SCF}} \mathcal{P}_{\text{SCF},i}^{\text{Sig}} \\ &\quad + (1 + Q_i A^{\text{Sig}}) f_{\text{Mis}} \mathcal{P}_{\text{Mis},i}^{\text{Sig}}] \\ &\quad + \sum_j N_j^{\text{Bkg}} \times \frac{1}{2} (1 - Q_i A_j^{\text{Bkg}}) \mathcal{P}_{j,i}^{\text{Bkg}}, \end{aligned}$$

where Q_i is the charge of the pion in the event, N^{Sig} (N_j^{Bkg}) and A^{Sig} (A_j^{Bkg}) are the yield and asymmetry for signal and background component j , respectively. The fractions of true signal (f_{Sig}), SCF signal (f_{SCF}), and wrong-charge mistag events (f_{Mis}) are fixed to the numbers obtained from MC simulations (Section 2). The j individual background terms comprise continuum, $b \rightarrow c$

decays, ρ^* , and 17 exclusive charmless B decay modes. The PDF for each component, in turn, is the product of the PDFs for each of the fit input variables, $\mathcal{P} = \mathcal{P}_{m_{ES}, \Delta E} \mathcal{P}_{ANN} \mathcal{P}_{m_{\pi\pi}}$. Due to correlations between ΔE and m_{ES} , the $\mathcal{P}_{m_{ES}, \Delta E}$ for signal and all background from B decays are described by two-dimensional non-parametric PDFs [13] obtained from MC events. For continuum background, $\mathcal{P}_{m_{ES}, \Delta E}$ is the product of two orthogonal one-dimensional parametric PDFs; m_{ES} is well described by an empirical phase-space threshold function [14] and ΔE is parameterized with a second degree polynomial. The parameters of the continuum PDFs are floated in the fit, with m_{ES} constrained to masses below $5.29 \text{ GeV}/c^2$. ANN is described by the product of an exponential and a polynomial function for continuum background and by a Crystal Ball function [15] for all other modes. For $\mathcal{P}_{m_{\pi\pi}}$, one-dimensional non-parametric PDFs obtained from MC events are used to describe all modes except the signal mode itself, which is described by a non-relativistic Breit-Wigner line-shape. The parameters for this PDF are held fixed to the MC values and varied within errors to estimate systematic uncertainties.

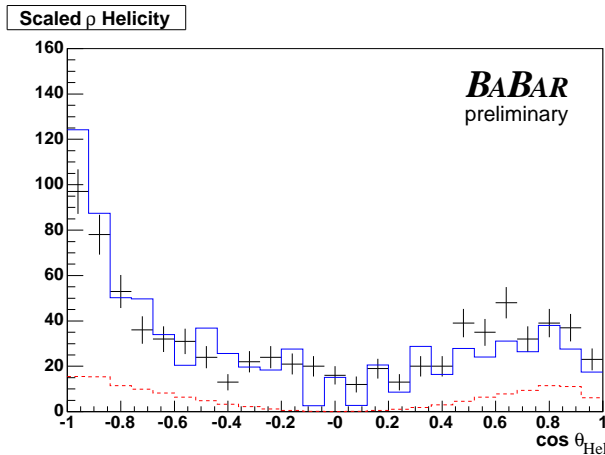


Figure 1: Distribution of $\cos \theta_{\text{Hel}}$ for $m_{ES} > 5.265$, $|\Delta E| < 0.1$, and $ANN > 0.85$. Data are shown in black, with error bars. The total PDF and the $B^\pm \rightarrow \rho^\pm \pi^0$ contribution are overlaid in solid blue and dashed red lines, respectively.

A number of cross checks confirm that the fit is unbiased. In 1000 separate MC pseudo-experiments we generate the expected number of events for the various fit components before using the maximum likelihood fit to extract the yields and asymmetries. The distributions for each component are generated from the component's PDF, giving values for the fit variables m_{ES} , ΔE , ANN , and $m_{\pi\pi}$. The expected number of events is calculated from the branching fraction and efficiency for each individual mode. The generated number of events for each fit component is determined by fluctuating the expected number according to a Poisson distribution. The test is repeated using samples with differing asymmetry values. We repeat these MC studies using fully simulated signal $B^\pm \rightarrow \rho^\pm \pi^0$ events instead of generating the signal component from our PDFs. This verifies that the signal component is correctly modeled including correlations between the fit variables. As another cross check we compare the distribution of the helicity angle θ_{Hel} between the momenta of the charged pion and the B -meson in the ρ rest frame in data with that modeled in MC samples for a variety of cuts. Fig. 1 shows the distribution of $\cos \theta_{\text{Hel}}$ for a pseudo-signal-box defined by $m_{ES} > 5.265$, $|\Delta E| < 0.1$, and $ANN > 0.8$. We generally find our PDFs in good

agreement with the data. Finally, omitting $m_{\pi\pi}$ as a fit variable has no significant influence on the signal yield, indicating that our treatment of ρ^* background is indeed effective.

5 Systematic Uncertainties

Table 2: Breakdown of systematic uncertainties.

Absolute uncertainties on yields	
Source	$\sigma_{\text{Syst.}}^{\text{Yield}}$ (Events)
Background normalization	+14.1 -13.4
PDF shapes	+ 4.7 - 4.2
SCF fraction	± 12.2
Mistag fraction	± 2.0
ΔE shift	± 2.6
Total	± 19
Relative uncertainties on $\mathcal{B}(B^\pm \rightarrow \rho^\pm \pi^0)$	
Source	$\sigma_{\text{Syst.}}^{\mathcal{B}}$ (%)
Efficiency estimation	± 7.3
B counting	± 1.1
Total	± 7.4
Uncertainties on \mathcal{A}_{CP}	
Source	$\sigma_{\text{Syst.}}^{\mathcal{A}_{CP}}$
Background normalization	± 0.006
Background asymmetry	± 0.024
PDF shapes	± 0.001
Total	± 0.02

Individual contributions to the systematic uncertainty are summarized in Table 2.

Absolute uncertainties on yields. We calculate the uncertainty of the continuum background estimation directly from the fit to data. The backgrounds from B decays are determined from simulation and fixed according to their efficiencies and branching fractions. The largest individual contribution comes from the $B \rightarrow a_1^0 \pi^0$ channel. For those individual decay modes which have been measured, we vary the number of events in the fit by their measured uncertainty. For all others we vary the amount included in the fit by $\pm 100\%$. For the $b \rightarrow c$ component, we fix the rate based on the number calculated from MC samples and vary the amount based on the statistical uncertainty of this number. The shifts in the fitted yields are calculated for each mode in turn and then added in quadrature to find the total systematic effect. The largest individual contribution comes from the ρ^* estimation.

To take into account the variation of the two-dimensional non-parametric PDFs used for ΔE and m_{ES} , we smear the MC-generated distributions from which the PDFs are derived. This is effectively done by varying the kernel bandwidth [13] up to twice its original value. For $m_{\pi\pi}$ and ANN , the parameterizations determined from fits to MC events are varied by one standard deviation. The systematic uncertainties are determined using the altered PDFs and fitting to the final data sample. The overall shifts in the central value are taken as the size of the systematic uncertainty.

We vary the SCF fraction by a conservative estimate of its relative uncertainty ($\pm 10\%$) and assign the shift in the fitted number of signal events as the systematic uncertainty of the SCF fraction.

To account for differences in the neutral particle reconstruction between data and MC simulation, the signal PDF distribution in ΔE is offset by ± 5 MeV and the data is then refitted. The larger of the two shifts in the central value of the yield is 2.2 events, which is taken as the systematic uncertainty for this effect.

Relative uncertainties on the branching fraction. Corrections to the π^0 energy resolution and efficiency, determined using various control samples, add a systematic uncertainty of 7.2%. A relative systematic uncertainty of 1% is assumed for the pion identification. A relative systematic uncertainty of 0.8% on the efficiency for a single charged track is applied. Adding all the above contributions in quadrature gives a relative systematic uncertainty on the branching fraction of 7.3%. Another contribution of 1.1% comes from the uncertainty on the total number of B events.

Uncertainties on the charge asymmetry. To calculate the effects of systematic shifts in the charge asymmetries of background modes, each mode is varied by its measured uncertainty. For contributions with no measurement, we assume zero asymmetry and assign an uncertainty of 20%, motivated by the largest charge asymmetry measured in any mode so far [16]. The individual shifts are then added in quadrature to find the total systematic uncertainty. In addition, the effect of altering the normalizations of the B backgrounds affects the fitted asymmetry. The size of the shift on the fitted \mathcal{A}_{CP} is taken as the size of the systematic uncertainty.

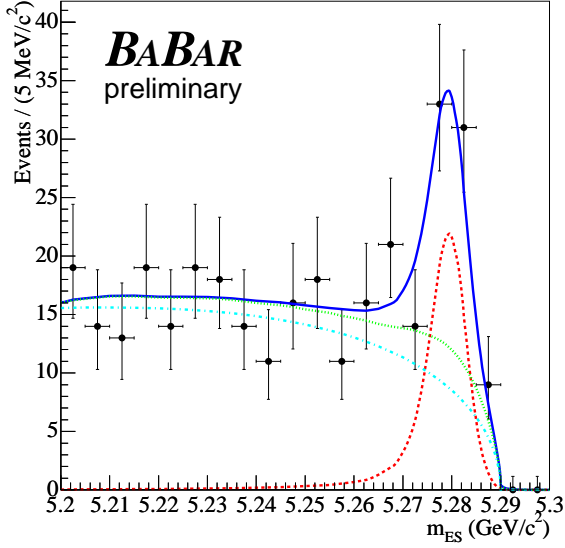
6 Results

The central value of the signal yield from the maximum likelihood fit is 357 ± 49 events, over 44840 ± 217 continuum events and an expected background of 872 ± 62 events from other B decays. We find a branching fraction and charge asymmetry of

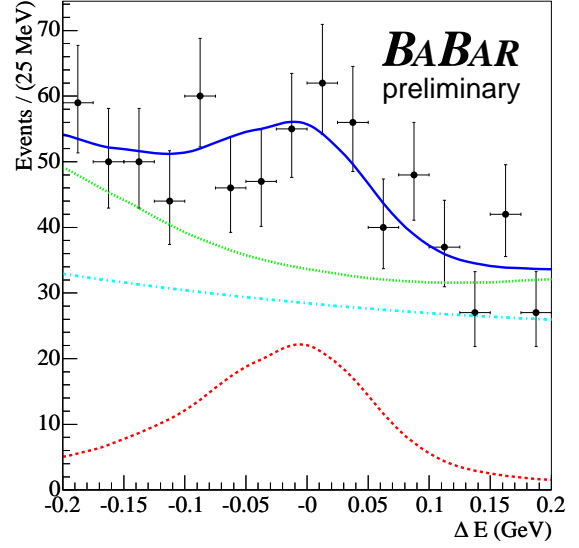
$$\begin{aligned} \mathcal{B}(B^\pm \rightarrow \rho^\pm \pi^0) &= [10.0 \pm 1.4 (Stat.) \pm 0.9 (Syst.)] \times 10^{-6} \\ \mathcal{A}_{CP}(B^\pm \rightarrow \rho^\pm \pi^0) &= -0.01 \pm 0.13 (Stat.) \pm 0.02 (Syst.). \end{aligned}$$

Compared against the null hypothesis, the statistical significance $\sqrt{-2 \ln(\mathcal{L}_{Null}/\mathcal{L}_{Max})}$ of the yield amounts to 8.7 standard deviations.

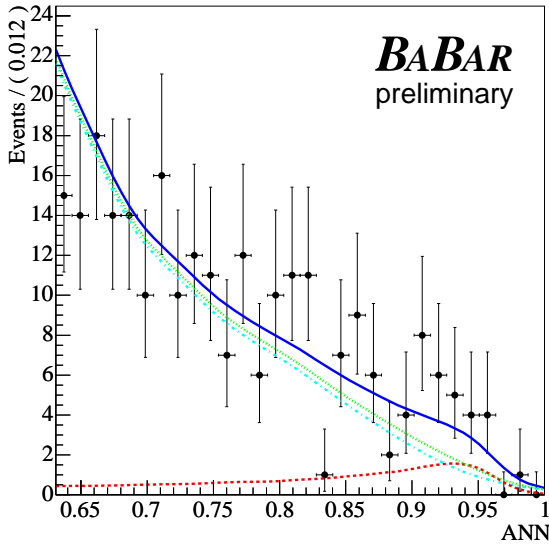
The results of the fit are illustrated in Fig. 2. The plots are enhanced in signal by selecting only those events which exceed a threshold of 0.1 (0.05 for ANN) for the likelihood ratio $R = (N^{Sig} \mathcal{P}^{Sig}) / (N^{Sig} \mathcal{P}^{Sig} + \sum_i N_i^{Bkg} \mathcal{P}_i^{Bkg})$, where N are the central values of the yields from the fit and \mathcal{P} are the PDFs with the projected variable integrated out. This threshold is optimized by maximizing the ratio $S = N^{Sig} \epsilon^{Sig} / \sqrt{N^{Sig} \epsilon^{Sig} + \sum_i N_i^{Bkg} \epsilon_i^{Bkg}}$ where ϵ are the efficiencies after the threshold is applied. The PDF components are then scaled by the appropriate ϵ .



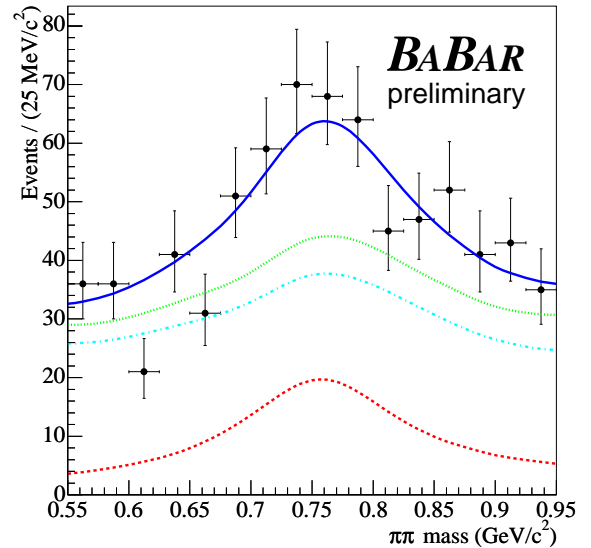
(a)



(b)



(c)



(d)

Figure 2: Likelihood projection plots for the four fit variables, (a) m_{ES} , (b) ΔE , (c) ANN , and (d) $m_{\pi\pi}$. In each plot the solid blue line represents the total PDF, the dotted green line represents the total background, the dotted-dashed light blue line represents the continuum contribution, and the dashed red line represents the signal component. The plots contain a subset of the events defined by a likelihood ratio of at least 0.1 (0.05 for ANN).

7 Conclusions

We have measured the branching fraction and charge asymmetry for the decay $B^\pm \rightarrow \rho^\pm \pi^0$ using a maximum likelihood fit. We obtain $\mathcal{B}(B^\pm \rightarrow \rho^\pm \pi^0) = [10.0 \pm 1.4 \pm 0.9] \times 10^{-6}$, and $\mathcal{A}_{CP} = -0.01 \pm 0.13 \pm 0.02$, respectively, where the first error is statistical and the second error systematic. The statistical significance of the signal is calculated to be 8.7 standard deviations. The results are in good agreement with the previous measurement [5].

Acknowledgements

We are grateful for the extraordinary contributions of our PEP-II colleagues in achieving the excellent luminosity and machine conditions that have made this work possible. The success of this project also relies critically on the expertise and dedication of the computing organizations that support *BABAR*. The collaborating institutions wish to thank SLAC for its support and the kind hospitality extended to them. This work is supported by the US Department of Energy and National Science Foundation, the Natural Sciences and Engineering Research Council (Canada), Institute of High Energy Physics (China), the Commissariat à l’Energie Atomique and Institut National de Physique Nucléaire et de Physique des Particules (France), the Bundesministerium für Bildung und Forschung and Deutsche Forschungsgemeinschaft (Germany), the Istituto Nazionale di Fisica Nucleare (Italy), the Foundation for Fundamental Research on Matter (The Netherlands), the Research Council of Norway, the Ministry of Science and Technology of the Russian Federation, and the Particle Physics and Astronomy Research Council (United Kingdom). Individuals have received support from CONACyT (Mexico), the A. P. Sloan Foundation, the Research Corporation, and the Alexander von Humboldt Foundation.

References

- [1] N. Cabibbo, *Phys. Rev. Lett.* **10**, 531 (1963).
- [2] M. Kobayashi and T. Maskawa, *Prog. Theor. Phys.* **49**, 652 (1973).
- [3] *BABAR* Collaboration, B. Aubert *et al.*, *Phys. Rev. Lett.* **91**, 201802 (2003).
- [4] A. Snyder and H. Quinn, *Phys. Rev. D* **48**, 2139 (1993).
- [5] *BABAR* Collaboration, B. Aubert *et al.*, *Phys. Rev. Lett.* **93**, 051802 (2004).
- [6] *BABAR* Collaboration, B. Aubert *et al.*, *Nucl. Instr. Methods Phys. Res., Sect. A* **479**, 1 (2002).
- [7] *BABAR* Collaboration, B. Aubert *et al.*, *Phys. Rev. D* **69**, 071101 (2004).
- [8] ARGUS Collaboration, A. Drescher *et al.*, *Nucl. Instr. Methods Phys. Res., Sect. A* **237**, 464 (1985).
- [9] *BABAR* Collaboration, B. Aubert *et al.*, *Phys. Rev. Lett.* **89**, 201802 (2002).
- [10] Particle Data Group, S. Eidelman *et al.*, *Phys. Lett. B* **592**, 1 (2004).
- [11] Heavy Flavor Averaging Group, J. Alexander *et al.*, hep-ex/0412073 (2004).

- [12] *BABAR* Collaboration, B. Aubert *et al.*, Phys. Rev. D **71**, 111101 (2005).
- [13] K. Cranmer, Comput. Phys. Commun. **136**, 198 (2001).
- [14] ARGUS Collaboration, H. Albrecht *et al.*, Phys. Lett. B **241**, 278 (1990).
- [15] T. Skwarnicki, *A Study of the Radiative Cascade Transitions Between the Υ' and Υ Resonances*, PhD thesis, Cracow Institute of Nuclear Physics, DESY-F31-86-02 (1986).
- [16] *BABAR* Collaboration, B. Aubert *et al.*, Phys. Rev. Lett. **93**, 131801 (2004).